

Klotho Depletion Contributes to Increased Inflammation in Kidney of the *db/db* Mouse Model of Diabetes via RelA (Serine)⁵³⁶ Phosphorylation

Yanhua Zhao,¹ Srijita Banerjee,¹ Nilay Dey,¹ Wanda S. LeJeune,¹ Partha S. Sarkar,² Reynolds Brobey,³ Kevin P. Rosenblatt,³ Ronald G. Tilton,^{1,4,5} and Sanjeev Choudhary^{1,5}

OBJECTIVE—Klotho is an antiaging hormone present in the kidney that extends the lifespan, regulates kidney function, and modulates cellular responses to oxidative stress. We investigated whether Klotho levels and signaling modulate inflammation in diabetic kidneys.

RESEARCH DESIGN AND METHODS—Renal Klotho expression was determined by quantitative real-time PCR and immunoblot analysis. Primary mouse tubular epithelial cells were treated with methylglyoxalated albumin, and Klotho expression and inflammatory cytokines were measured. Nuclear factor (NF)- κ B activation was assessed by treating human embryonic kidney (HEK) 293 and HK-2 cells with tumor necrosis factor (TNF)- α in the presence or absence of Klotho, followed by immunoblot analysis to evaluate inhibitor of κ B (I κ B) α degradation, I κ B kinase (IKK) and p38 activation, RelA nuclear translocation, and phosphorylation. A chromatin immunoprecipitation assay was performed to analyze the effects of Klotho signaling on interleukin-8 and monocyte chemoattractant protein-1 promoter recruitment of RelA and RelA serine (Ser)⁵³⁶.

RESULTS—Renal Klotho mRNA and protein were significantly decreased in *db/db* mice, and a similar decline was observed in the primary cultures of mouse tubule epithelial cells treated with methylglyoxal-modified albumin. The exogenous addition of soluble Klotho or overexpression of membranous Klotho in tissue culture suppressed NF- κ B activation and subsequent production of inflammatory cytokines in response to TNF- α stimulation. Klotho specifically inhibited RelA Ser⁵³⁶ phosphorylation as well as promoter DNA binding of this phosphorylated form of RelA without affecting IKK-mediated I κ B α degradation, total RelA nuclear translocation, and total RelA DNA binding.

CONCLUSIONS—These findings suggest that Klotho serves as an anti-inflammatory modulator, negatively regulating the production of NF- κ B-linked inflammatory proteins via a mechanism that involves phosphorylation of Ser⁵³⁶ in the transactivation domain of RelA. *Diabetes* 60:1907–1916, 2011

From the ¹Department of Internal Medicine, University of Texas Medical Branch, Galveston, Texas; the ²Department of Neurology, Neuroscience, and Cell Biology, University of Texas Medical Branch, Galveston, Texas; the ³Brown Foundation Institute of Molecular Medicine, University of Texas Health Science Center, Houston, Texas; the ⁴Department of Ophthalmology and Visual Sciences, University of Texas Medical Branch, Galveston, Texas; and the ⁵Sealy Center for Molecular Medicine, University of Texas Medical Branch, Galveston, Texas.

Corresponding author: Sanjeev Choudhary, sachoudh@utmb.edu.

Received 7 September 2010 and accepted 10 April 2011.

DOI: 10.2337/db10-1262

This article contains Supplementary Data online at <http://diabetes.diabetesjournals.org/lookup/suppl/doi:10.2337/db10-1262/-/DC1>.

Y.Z. and S.B. contributed equally to this study.

© 2011 by the American Diabetes Association. Readers may use this article as long as the work is properly cited, the use is educational and not for profit, and the work is not altered. See <http://creativecommons.org/licenses/by-nc-nd/3.0/> for details.

It has long been recognized that diabetes accelerates aging, particularly in the subpopulation of diabetic subjects who are at risk for developing complications (1). Numerous mechanisms have been proposed, including increased production of advanced glycation end products (AGEs), increased oxidative stress, DNA damage, and enhanced inflammation; it is noteworthy that all of these mechanisms have been implicated in the pathogenesis of diabetes complications. Tubular epithelium in the kidneys from type 2 diabetic patients with demonstrated nephropathy display accelerated senescence, characterized by decreased telomere length and an increased expression of senescence markers (2).

The recent characterization of the Klotho protein as an antiaging hormone that modulates the expression level of antioxidant enzymes (3,4), as well as its high expression level in the kidney (5–7), suggest that Klotho plays a role in accelerated aging and cellular senescence observed in diabetes. Klotho overexpression extends the mouse lifespan by 20–30% (8). More striking, Klotho-deficient mice exhibit multiple age-related phenotypes and succumb to early, premature death (7,9). Klotho is predominantly expressed in the brain and kidney of normal subjects, and a significant decline in *Klotho* gene and protein expression has been reported in kidneys of patients with chronic renal failure (10). Klotho expression is significantly suppressed after the induction of renal ischemia-reperfusion injury, whereas Klotho overexpression prevented the development of acute renal failure (11). Also noteworthy, Klotho overexpression suppressed glomerulonephritis-induced accelerated cellular senescence and apoptosis and preserved renal function (12). Despite these observations, the role of Klotho in diabetes remains unexplored, even though accelerated aging is associated with this disease.

We investigated potential links between Klotho expression and diabetes-induced inflammation. Our data show that Klotho suppresses nuclear factor (NF)- κ B activation and the subsequent production of inflammatory cytokines in response to tumor necrosis factor (TNF)- α stimulation in kidney cells, including primary cultures of mouse tubular epithelium, HK-2, and human embryonic kidney (HEK) 293 cells. We explored potential mechanism(s) for this inhibition and identified a novel and specific site of inhibition. Klotho inhibited p38 kinase and specifically blocked RelA serine (Ser)⁵³⁶ phosphorylation and its subsequent recruitment to NF- κ B-dependent promoters of multiple cytokines, without affecting inhibitor of κ B (I κ B) α degradation or total RelA nuclear translocation and DNA binding. These findings indicate that Klotho serves as

an anti-inflammatory modulator, regulating the production of NF- κ B-linked inflammatory cytokines, chemokines, and growth factors via a noncanonical NF- κ B activation pathway involving RelA phosphorylation in the transactivation domain (13–15). Our observations that Klotho can modulate NF- κ B activation and inhibit the production of diabetes-induced inflammatory cytokines suggest that Klotho exerts a renoprotective effect by increasing the resistance to oxidative stress and inhibiting inflammatory cytokine/chemokine cascades induced by NF- κ B activation. Our observations further suggest that Klotho is a potential therapeutic target linking oxidative stress to inflammation in type 2 diabetes.

RESEARCH DESIGN AND METHODS

Animal and surgical protocols. Male *Lepr^{db} (db/db)* and control mice with the same genetic background (C57BLKS/J) were purchased from The Jackson Laboratories (Bar Harbor, ME) and housed in the University of Texas Medical Branch Animal Resource Center in a room with a 12-h light cycle and with free access to standard diet and water. The animals were cared for in accordance with the University of Texas Medical Branch Institutional Animal Care and Use Committee policies and the *Public Health Service Guide for the Care and Use of Laboratory Animals*. At 20 weeks of age, the mice were anesthetized (70/10 mg/kg i.p. ketamine/xylazine), anticoagulated (5 units heparin), then exsanguinated prior to rapid aortic perfusion with ice-cold PBS to quickly rinse kidneys free of blood and to deliver a protease inhibitor cocktail (P8340; Sigma), phosphatase (1 mmol/L orthovanadate and 30 mmol/L sodium fluoride) inhibitors, and dithiothreitol (0.5 mmol/L). Both kidneys were removed, decapsulated, flash frozen in liquid nitrogen, then stored at -80°C until they were processed for protein or RNA extraction. A coronal section through the midline of one kidney at the level of the renal pelvis was fixed in 4%

paraformaldehyde for 24 h, transferred to Hanks' balanced salt solution, and stored at 4°C until it was processed for immunohistochemistry.

Isolation and primary culture of renal tubular epithelial cells. Renal cortical tubular epithelial cells were isolated and cultured using published techniques with modifications (16). In brief, 12- to 16-week-old C57BL/6 male mice were used to prepare primary renal proximal tubule cell cultures. Kidneys were sliced into coronal sections, and the renal cortex was dissected from the medulla, minced, and then washed three times in ice-cold Dulbecco's modified Eagle's medium (DMEM)/F12 media containing 0.1% BSA, followed by enzymatic digestion using 1% Worthington collagenase type II and 0.25% soybean trypsin inhibitor. Cell suspensions were passed through 200 mesh filters followed by 325 mesh filters then resuspended in 45% Percoll and centrifuged at 26,891g for 15 min at 4°C . Proximal tubule cells were sedimented to a layer immediately above the erythrocyte pellet. Proximal tubule cells were removed, centrifuged, washed to remove the remaining Percoll, and then resuspended in DMEM/F-12 containing 50 units/mL penicillin, 50 $\mu\text{g}/\text{mL}$ streptomycin, 10 ng/mL epidermal growth factor, 0.5 $\mu\text{mol}/\text{L}$ hydrocortisone, 0.87 $\mu\text{mol}/\text{L}$ bovine insulin, 50 $\mu\text{mol}/\text{L}$ prostaglandin E₁, 50 nmol/L sodium selenite, 50 $\mu\text{g}/\text{mL}$ human transferrin, and 5 pmol/L 3,3',5-triiodo-L-thyronine. Cells were plated on Matrigel-coated cover slips, or plastic cell-culture dishes coated with Matrigel, and maintained in an incubator at 37°C in 5% CO_2 . Cultures were left undisturbed for 48 h, after which culture media was replaced every 2 days until cells achieved confluence. For all experiments, cells were used within five passages, as described (16).

Cell culture. Human kidney cortex proximal tubular cells, HK-2 (American Type Culture Collection), were grown and maintained in the recommended medium, DMEM/Ham's F12 (50/50) supplemented with 10% FBS, L-glutamine, insulin, transferrin, sodium selenite, epidermal growth factor (2.5 ng/mL), and pituitary extract (1.5 $\mu\text{g}/\text{mL}$) in a humidified atmosphere of 5% CO_2 . HEK epithelial cells, (HEK293) were cultured in MEM media with 10% FBS, non-essential amino acids, sodium pyruvate, and antibiotics in a humidified atmosphere of 5% CO_2 .

Transient transfection and luciferase activity assay. Transient transfection using lipofectamine PLUS reagent (Invitrogen) was performed in

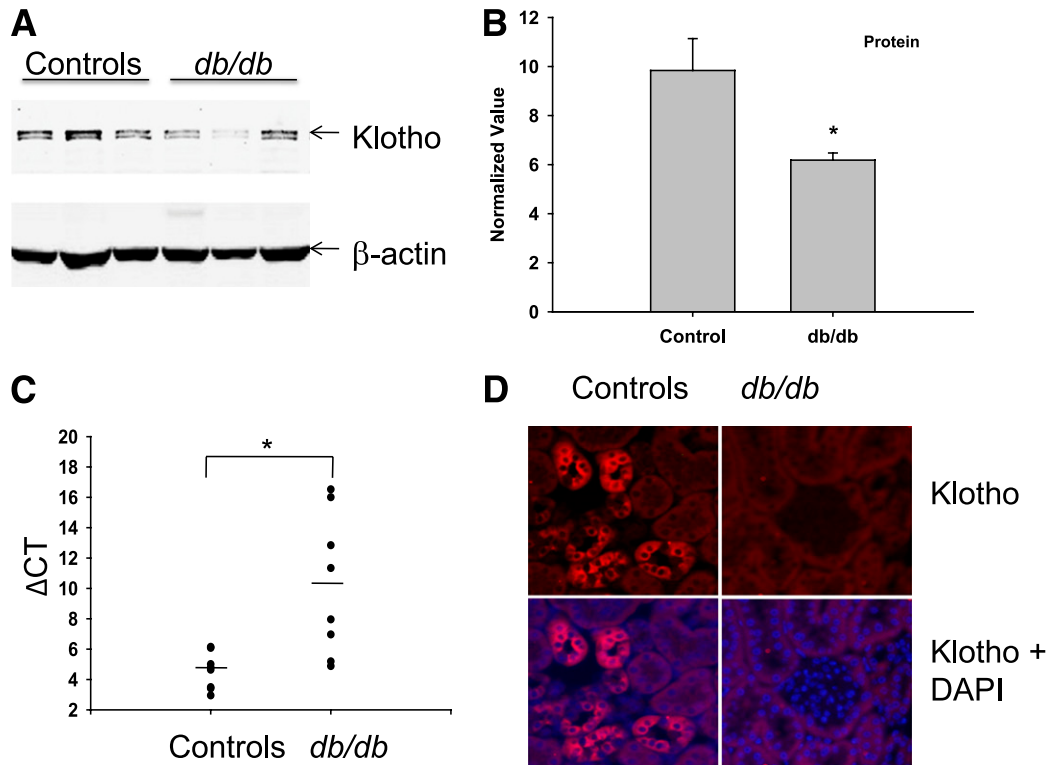


FIG. 1. Diabetes decreases Klotho protein and message in *db/db* mice. Kidney cortex from eight control mice and eight *db/db* mice were lysed in radioimmunoprecipitation assay buffer for protein or in trizol reagent for RNA extraction. **A:** Representative Western blots probed with anti-Klotho antibody (*upper panel*) and normalized to β -actin as loading controls (*lower panel*). **B:** Immunoblotted Klotho and respective β -actin bands from eight mice were quantified using a Licor Image Analyzer and normalized to β -actin. Data are means \pm SD of normalized arbitrary scan values. **C:** A decline in Klotho transcript, as measured by semiquantitative real-time PCR, is shown. Relative quantification of Klotho mRNA was performed using a MyiQ Single-Color Real-Time PCR Detection System and iQ SYBR Green Supermix, according to the manufacturer's instructions. Data were analyzed using the ΔC_T method in reference to GAPDH. $n = 8$ controls; $n = 8$ *db/db* mice. Significantly different from controls by Student *t* test: $*P < 0.05$. **D:** Kidney sections from control and *db/db* mice were stained with anti-Klotho antibody (*upper panel*) and counterstained with DAPI for nuclear staining (*lower panel*). (A high-quality digital representation of this figure is available in the online issue.)

triplicate plates according to the manufacturer's instructions. Cells were plated into six-well plates and transfected with 2 μg of construct with a NF- κB -LUC reporter gene. A total of 48 h after transfection, cells were pretreated with different concentrations of Klotho (50–200 pmol/L) for 45 min prior to TNF- α (20 ng/mL) stimulation for 6 h. Cells were lysed, and luciferase activity was measured using a luminometer. Values were normalized to untreated empty vector-transfected cells and expressed as fold change over control.

Preparation of methylglyoxal-modified serum albumin. Human serum albumin (HSA) minimally modified by methylglyoxal was prepared by incubation of the protein (100 $\mu\text{mol/L}$) in sodium phosphate buffer (100 mmol/L [pH 7.4] and 37°C) with 500 $\mu\text{mol/L}$ methylglyoxal for 24 h, followed by dialysis of the modified protein against ammonium bicarbonate buffer (30 mmol/L [pH 7.9] and 4°C) for 24 h, and then the dialysis buffer was changed to PBS for another 24 h. The modified albumin was sterilized by filtration (0.22 μm) before aliquoting and storage at -80°C . Unmodified protein was processed similarly for control experiments by excluding the 500 $\mu\text{mol/L}$ methylglyoxal. All reagents used in the preparation of methylglyoxal-modified human serum albumin (MG-HSA) were endotoxin free. The extent of modification was determined by amino acid analysis, and <15% modification was used in this study, as reported earlier (17). Negligible levels of endotoxin were detected in methylglyoxal-modified human serum albumin (MG-HSA) (0.0019 endotoxin units [EU]/mL), and control HSA (0.0029 EU/mL) was determined using a commercially available kit (GenScript, Piscataway, NJ).

Cytokine measurements. Multiple cytokines and chemokines were measured on aliquots of culture media or cell extracts collected after MG-HSA or TNF treatment using the Bio-Plex system, which is a multiplex bead-based assay used with the Luminex xMAP technology, according to the manufacturer's instructions (Bio-Rad Laboratories, Hercules, CA). Eight-point standard curves were performed for each cytokine using the same Luminex bead technology.

Preparation of subcellular extracts. Cells were harvested in PBS, centrifuged, and the pellets resuspended sequentially in low-salt, sucrose, and high-salt solutions to obtain cytosolic and highly purified nuclear extracts as previously described (18). Protein concentrations were measured by Coomassie dye binding (protein reagent; Bio-Rad Laboratories). Efficiency of separation of

cytosolic and nuclear proteins was assayed by Western blotting and probing both samples for cytosolic (β -tubulin and glyceraldehyde-3-phosphate dehydrogenase [GAPDH]) and nuclear (lamin B) proteins.

Western immunoblotting. Proteins were fractionated by SDS-PAGE and transferred to nitrocellulose or polyvinylidene difluoride membranes (Millipore, Bedford, MA). Membranes were blocked in 5% milk or 5% BSA for 0.5–1 h and then incubated with the indicated primary antibody at 4°C overnight. Membranes were washed in Tris-buffered saline, 0.1% Tween 20, and incubated with secondary antibody at 20°C for 1 h. Signals were visualized by the Odyssey Infrared Imaging System using fluorescent secondary antibodies or with an enhanced chemiluminescent (ECL) system onto film. β -Actin was used as a loading control.

Quantitative real-time PCR. Total cellular RNA was extracted using Tri Reagent (Sigma). A total of 2 μg RNA was used for reverse transcription using the SuperScript III First-Strand Synthesis System from Invitrogen (Carlsbad, CA). A total of 2 μL cDNA products were amplified in a 20- μL reaction system containing 10 μL iQ SYBR Green Supermix (Bio-Rad) and 400 nmol/L primer mixture. Relevant primers were purchased from SA Bioscience (Frederick, MD). All reactions were processed in a MyiQ Single Color Real-Time PCR thermocycler using a two-step-plus-melting curve program. Results were analyzed by the iQ5 program (Bio-Rad), and the data were analyzed using the ΔC_T method in reference to GAPDH (19).

Chromatin immunoprecipitation assay. The chromatin immunoprecipitation (ChIP) assay was performed as described (20). In brief, $4\text{--}6 \times 10^6$ cells were sequentially cross-linked with disuccinimidyl glutarate (Thermo Scientific, Rockford, IL) and 1% formaldehyde in PBS, solubilized in 500 μL SDS lysis buffer (1% SDS; 50 mmol/L Tris [pH 8.0]; and 10 mmol/L EDTA) with a protease inhibitor cocktail (Sigma-Aldrich), and chromatin sheared by sonication. Equal amounts of DNA were immunoprecipitated overnight at 4°C with 4 μg of indicated antibody. Anti-RelA (sc-372) or IgG (as negative control) were obtained from Santa Cruz (Santa Cruz, CA). Antiphospho-serine⁵³⁶ RelA antibodies were from Cell Signaling (catalog no. 3031; Danvers, MA). Immunoprecipitates were collected with protein A magnetic beads (Invitrogen). Eluted DNA was de-cross-linked and used as a template in real-time-PCR. Primers for amplifying the interleukin (IL)-8 promoter were AGGTTTGGCCCTGAGGGGATG (F) and

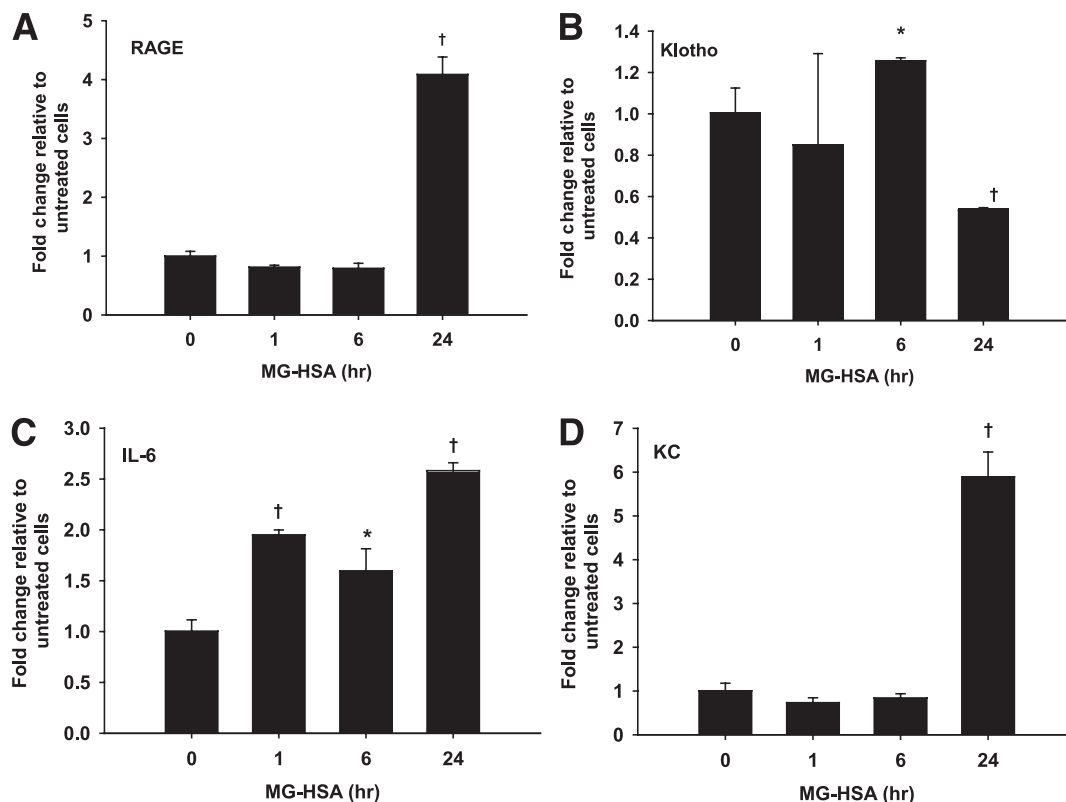


FIG. 2. MG-HSA induces Klotho depletion and increases cytokine production. Renal primary tubular epithelial cells were treated with MG-HSA (5 $\mu\text{mol/L}$) for various times, and expression levels of Klotho (A), RAGE (B), IL-6 (C), and KC (D) were measured by using quantitative RT-PCR. Data were normalized to GAPDH and expressed as fold change, compared with the untreated cells (0 time interval). Data represent the means \pm SD of three independent experiments and were compared using one-way ANOVA with multiple comparisons, followed by the Tukey post hoc test for significance between time intervals. * $P < 0.01$ and † $P < 0.0001$ were significantly different than untreated cells.

GGAGTGTCTCCGGTGGCTTTT (R). For the monocyte chemoattractant protein (MCP)-1 promoter, the primer sequences were CTGCTTCCCTTCTCTACT (F) and ATCTTCCATGAGTGATAAGTG (R).

Statistical analysis. Data are reported as means \pm SD. Because all data were normally distributed on the basis of the Kolmogorov-Smirnov test, both one-way and two-way ANOVA tests were performed to evaluate overall group differences. This was followed by the Tukey post hoc test to determine pairwise significance if the ANOVA test indicated that a significant difference was present in the dataset. In the case of only two group comparisons, a two-sample Student *t* test was performed after checking for variance distribution via the Levene test. In all cases, *P* < 0.05 was considered significant.

RESULTS

Diabetes reduces renal cortical Klotho transcript and protein levels. As shown in Fig. 1, renal cortical Klotho protein (by immunoblot) and RNA message (by quantitative RT-PCR) levels in *db/db* mice were decreased significantly at 20 weeks of age (after \sim 12 weeks of hyperglycemia). Despite heterogeneity in protein expression levels within each group (Fig. 1A), we observed a 50% decrease in Klotho protein in the *db/db* group compared with age- and sex-matched controls (Fig. 1B). We observed a significant decline (*P* < 0.01) in Klotho message (mean ΔC_T = 10.4) in the diabetic renal cortex compared with the control renal cortex (mean ΔC_T = 4.5) (Fig. 1C), suggesting that the decline in Klotho protein expression resulted from suppressed *Klotho* gene expression. Klotho was predominantly expressed in tubules but not in the glomeruli of control mice, with less Klotho immunostaining evident in diabetic kidneys (Fig. 1D).

AGEs (MG-HSA) induce the loss of Klotho expression and increase cytokine expression in the primary cultures of renal tubular epithelium. We previously have reported noncanonical NF- κ B pathway activation in the renal cortex of *db/db* mice, with a several-fold increase in NF- κ B-inducing kinase (NIK) expression, a key enzyme regulating activation of this particular NF- κ B pathway (18). Because both Klotho and NIK are predominantly expressed in renal tubules (6,21), we explored the possibility that increased NF- κ B activation and cytokine production in the renal tubules of *db/db* mice are linked to the decline of Klotho. Renal tubular epithelial cells were isolated from C57BL/6 mice, and immunofluorescence microscopy was used to check the purity of the enriched tubular epithelial cell preparation (see Supplementary Fig. 1). Primary cultures of enriched tubular epithelial cells were exposed to MG-HSA (5 μ mol/L) for 1–24 h followed by RNA isolation with the trizol reagent. As shown in Fig. 2A and B, 24 h of MG-HSA treatment resulted in a fourfold increase in the expression of the receptor for AGEs (RAGEs) and a 50% decline in Klotho levels similar to the decline observed in vivo. MG-HSA treatment produced a significant increase in proinflammatory cytokine mRNA expression for IL-6 (Fig. 2C) and keratinocyte chemoattractant (KC), the mouse ortholog of IL-8 (Fig. 2D), as well as increased protein levels for these cytokines in culture media (Supplementary Fig. 2). The time course of KC production was similar to RAGEs, whereas IL-6 began to increase within 1 h. These experiments suggest that primary renal tubular cells respond to MG-HSA by inducing RAGE expression and increased cytokine production and that a diabetic stimulus, such as MG-HSA, can suppress Klotho expression. Taken together, these experiments indicate that the diabetic milieu decreases renal Klotho levels, which may be linked to diabetes-induced inflammation.

Klotho inhibits NF- κ B promoter activity. Because the loss of Klotho in diabetic kidneys could lead to activation

of NF- κ B, we investigated whether Klotho negatively regulates NF- κ B pathway activity. HEK293 cells were first transfected with the luciferase plasmid containing the consensus NF- κ B sequence followed by 45 min of preincubation with different concentrations of exogenously added Klotho prior to TNF- α (20 ng/mL) treatment for 6 h, as previously described (4). Exogenous addition of Klotho inhibited NF- κ B-dependent promoter activity in a dose-dependent manner, with an \sim 70% inhibition observed at 200 pmol/L (Fig. 3A). Klotho was used at this concentration in subsequent experiments. Klotho also had some inhibitory effects on basal NF- κ B activation in the absence of TNF- α stimulation (Fig. 3B), suggesting that it might have a constitutive anti-inflammatory role in cells.

Klotho inhibits TNF- α -induced cytokine production. To further ascertain the inhibitory effect of Klotho on NF- κ B activation, HEK293 cells were preincubated with 200 pmol/L Klotho for 45 min prior to TNF- α (20 ng/mL) treatment for 1 h; then the cells were lysed in trizol reagent and the extracted RNA was used for quantitative RT-PCR. Klotho significantly inhibited TNF- α -induced IL-8, IL-6, regulated upon activation normal T-cell expressed, and presumably secreted (RANTES), and MCP-1 production (Fig. 4), although to different extents, which may reflect differences in their kinetics and efficacies of induction by

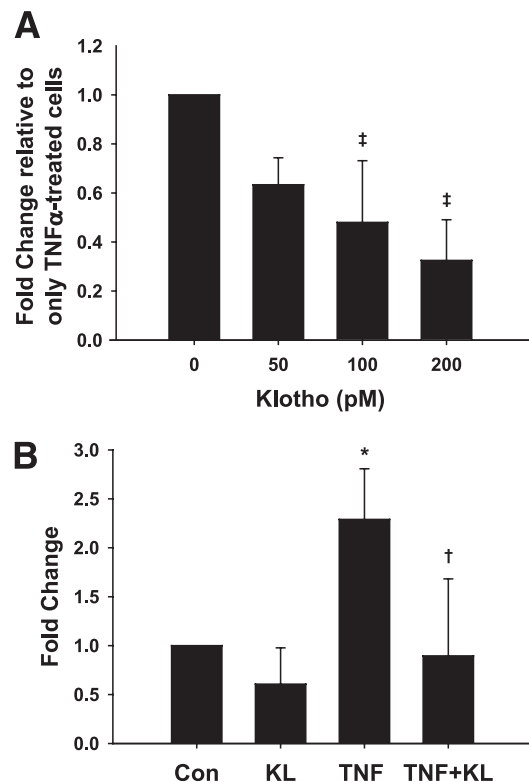


FIG. 3. Klotho (KL) inhibits TNF- α -induced, NF- κ B-dependent promoter activity. **A:** Dose curve of Klotho inhibition. HEK293 cells expressing NF- κ B-dependent luciferase were preincubated with different concentrations of Klotho for 45 min before stimulating with TNF- α (20 ng/mL) for 6 h. Values were plotted as fold inhibition compared with TNF- α -treated cells in the absence of Klotho. **B:** A total of 200 pmol per mL Klotho significantly inhibited TNF- α -induced NF- κ B activation. Data represent the means \pm SD of three independent experiments and were analyzed by one-way ANOVA, followed by a Tukey post hoc test for significance between doses (A) and multiple treatment groups (B). **P* < 0.05 is significantly different than controls (CON); †*P* < 0.06 and ‡*P* < 0.01 are significantly different than TNF- α -treated samples.

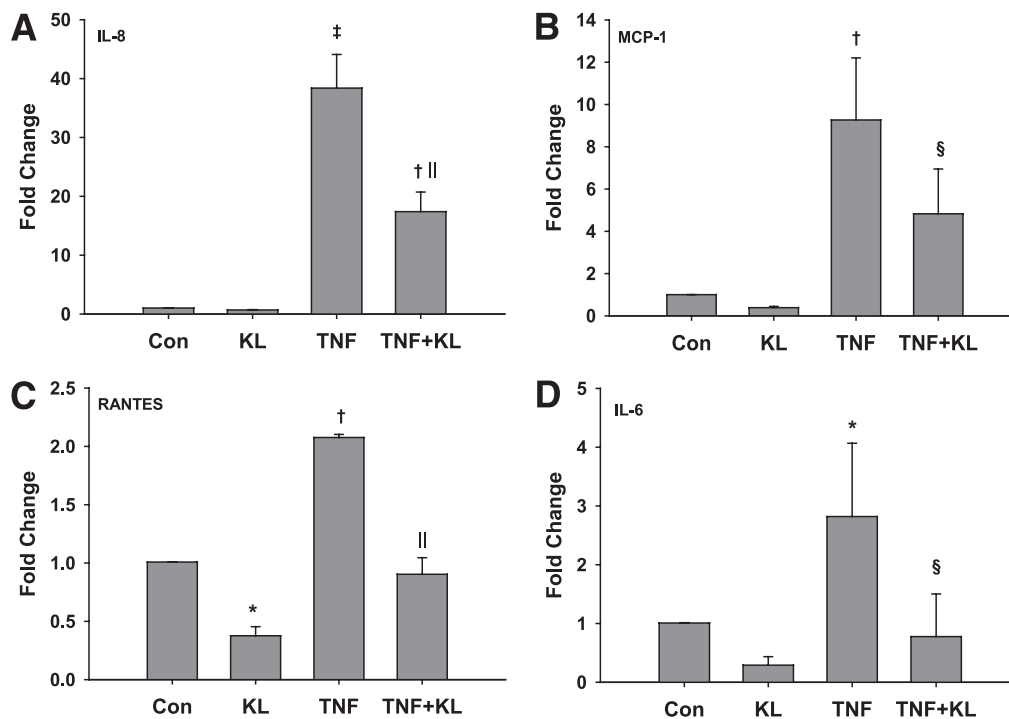


FIG. 4. Klotho (KL) inhibits NF- κ B-dependent cytokine production. HEK293 cells were treated with TNF- α in the presence of Klotho, and the effect of Klotho on TNF- α -induced cytokine expression was examined by quantitative RT-PCR using cytokine-specific primers and normalized to GAPDH as the internal control. Fold change was calculated by comparing the values to their respective untreated controls (CON). Data represent the means \pm SD of three independent experiments, and overall significance was determined using one-way ANOVA. Significance between groups was analyzed by performing a Turkey post hoc test. * $P < 0.05$, † $P < 0.005$, and ‡ $P < 0.0001$ were significantly different than control samples, whereas § $P < 0.05$ and || $P < 0.0001$ were significantly different than TNF- α -treated samples.

TNF- α . To rule out the possibility that exogenously added Klotho might interfere with TNF- α binding to its receptor, thereby inhibiting NF- κ B activation and cytokine production, Klotho was transiently overexpressed in HK-2 cells. These cells were treated with TNF- α (20 ng/mL) for different time intervals. Figure 5A and B shows that overexpressed Klotho completely inhibited MCP-1 expression at all time intervals and significantly inhibited IL-8 expression up to 6 h. MCP-1 and IL-8 levels also were measured in culture media (Fig. 5C and D) and cell lysates (Fig. 5E and F). For these experiments, cells expressing Klotho or vector were exposed to TNF- α for 6 h prior to cytokine measurement by enzyme-linked immunosorbent assay. Although Klotho overexpression significantly reduced IL-8 in both culture media and cell lysates, MCP-1 production was significantly reduced only in culture media and did not reach statistical significance in cell lysates ($P = 0.08$). Supplementary Fig. 3 shows the induced expression level of Klotho in these cells. Thus, Klotho-mediated inhibition of TNF- α -induced NF- κ B activation is a cellular event and not the physical interference of TNF- α binding to its receptor.

Klotho inhibits TNF- α -induced RelA (Ser)⁵³⁶ phosphorylation. To further explore mechanism(s) of Klotho-mediated inhibition of TNF- α -induced NF- κ B activation, we investigated the impact of Klotho on cytoplasmic and nuclear events in NF- κ B activation. Figure 6A and Supplementary Fig. 4 show similar TNF- α -induced cytosolic I κ B α degradation in the presence and absence of Klotho, suggesting that Klotho has no effect on I κ B kinase (IKK) activation of the NF- κ B canonical pathway. Next, we quantified nuclear translocation of total RelA after TNF- α treatment for 30 min. This experiment demonstrated that increased RelA nuclear accumulation in response to TNF- α was

unaffected by Klotho treatment (Fig. 6B, top panel and Supplementary Fig. 5). However, when immunoblotted for RelA (Ser)⁵³⁶ phosphorylation, Klotho blocked this phosphorylation event in the cytoplasm and to a lesser, but still significant, extent in the nucleus (Fig. 6B, middle panel). Figures 6C and D provide quantitation of RelA (Ser)⁵³⁶ immunoblots from three independent experiments. These results suggest that Klotho specifically blocked a non-canonical NF- κ B activation pathway mediated by RelA (Ser)⁵³⁶ phosphorylation and did not inhibit the IKK-dependent classical NF- κ B activation pathway.

Klotho inhibits p38 kinase. Although several kinases have been reported to phosphorylate RelA at Ser⁵³⁶ in response to various stimuli (22), IKK β and phosphoinositide 3-kinase (PI3K)/Akt seem to be the predominant kinases involved. Because Klotho had no effect on TNF- α -induced I κ B α degradation, IKK β may not be a site of action of Klotho. However, earlier reports have shown that the exogenous addition of Klotho significantly reduced Akt phosphorylation (4). Moreover, RelA (Ser)⁵³⁶ phosphorylation by Akt has been reported to be mediated via p38 activation (23). Therefore, we investigated if Klotho inhibits p38 phosphorylation. HEK293 cells were treated with TNF- α (20 ng/mL for 1 h), and p38 phosphorylation was examined by immunoblotting. TNF- α treatment increased p38 phosphorylation compared with untreated cells (Fig. 7A, upper panel), and pretreatment with Klotho significantly reduced the TNF- α -induced phosphorylation. Immunoblots from three independent experiments were quantitated and normalized to total p38 and expressed as fold change versus control cells (Fig. 7A, lower panel). We also investigated if Klotho inhibited IKK α , another RelA (Ser)⁵³⁶ kinase. Although 30 min of TNF- α treatment

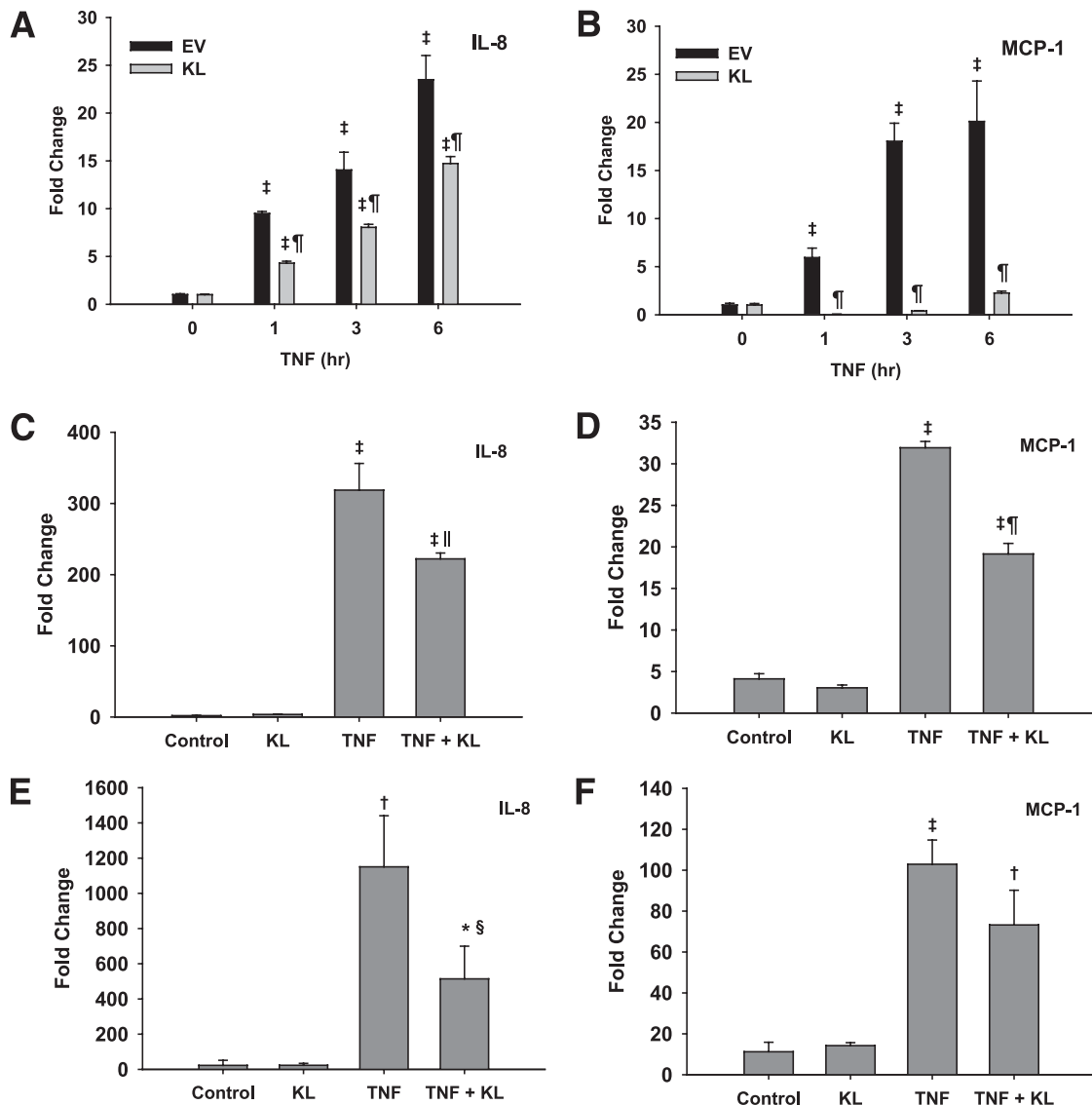


FIG. 5. Overexpression of Klotho (KL) inhibits MCP-1 and IL-8 expression. HK-2 cells expressing empty vector (EV) or Klotho were treated with TNF- α (20 ng/mL) for 1–6 h before performing quantitative RT-PCR using IL-8- and MCP-1-specific primers. Data were normalized to the respective GAPDH and expressed as fold change compared with untreated cells (A and B). Cells were treated with TNF- α for 6 h before measuring cytokine levels in culture media (C and D) and cell lysates (E and F) by enzyme-linked immunosorbent assay. Values were normalized to total protein and expressed as fold change to vector-transfected control cells. Data represent the means \pm SD of three independent experiments and were analyzed by two-way ANOVA with multiple comparison (time and treatment) and the Tukey post hoc test for significance between time intervals and the treatment groups. * $P < 0.05$, † $P < 0.005$, and ‡ $P < 0.0001$ were significantly different from control samples. § $P < 0.05$, || $P < 0.001$, and ¶ $P < 0.0001$ were significantly different from TNF- α -treated samples.

increased p -IKK α levels, as demonstrated by immunoblot, exogenously added Klotho failed to inhibit the phosphorylation (Fig. 7B and Supplementary Fig. 6).

Klotho inhibits TNF- α -induced recruitment of phospho-RelA (Ser)⁵³⁶ on IL-8 and MCP-1 promoters. We investigated whether Klotho inhibition of RelA phosphorylation affected its recruitment onto NF- κ B-dependent promoters, leading to inhibition of cytokine production. HEK293 cells were pretreated with Klotho (200 pmol/L) for 45 min and then stimulated with TNF- α (20 ng/mL) for 30 min. Recruitment of either total RelA or phospho-RelA (Ser)⁵³⁶ onto IL-8 and MCP-1 promoters was evaluated by the ChIP assay. Figure 8A shows a strong induction of total RelA as well as phospho-RelA (Ser)⁵³⁶ binding on the MCP-1 promoter after 30 min of TNF- α treatment, whereas Klotho pretreatment in the absence of TNF- α

had no significant effect on their promoter binding. Klotho treatment significantly reduced phospho-RelA (Ser)⁵³⁶ binding induced by TNF- α (Fig. 8A, lower panel) without significantly affecting total RelA binding to the MCP-1 promoter. Similar results were obtained using the IL-8 promoter (Fig. 8B). Supplementary Fig. 7 shows a representative gel from these experiments depicting the similar changes in the RelA and RelA (Ser)⁵³⁶ recruitment on both the promoters. These results indicate that Klotho did not inhibit TNF- α -induced RelA nuclear translocation and relevant promoter binding but specifically blocked RelA (serine)⁵³⁶ phosphorylation and its binding to NF- κ B-dependent promoters and further suggest that the anti-inflammatory effects of Klotho are mediated via inhibition of this NF- κ B noncanonical activation pathway.

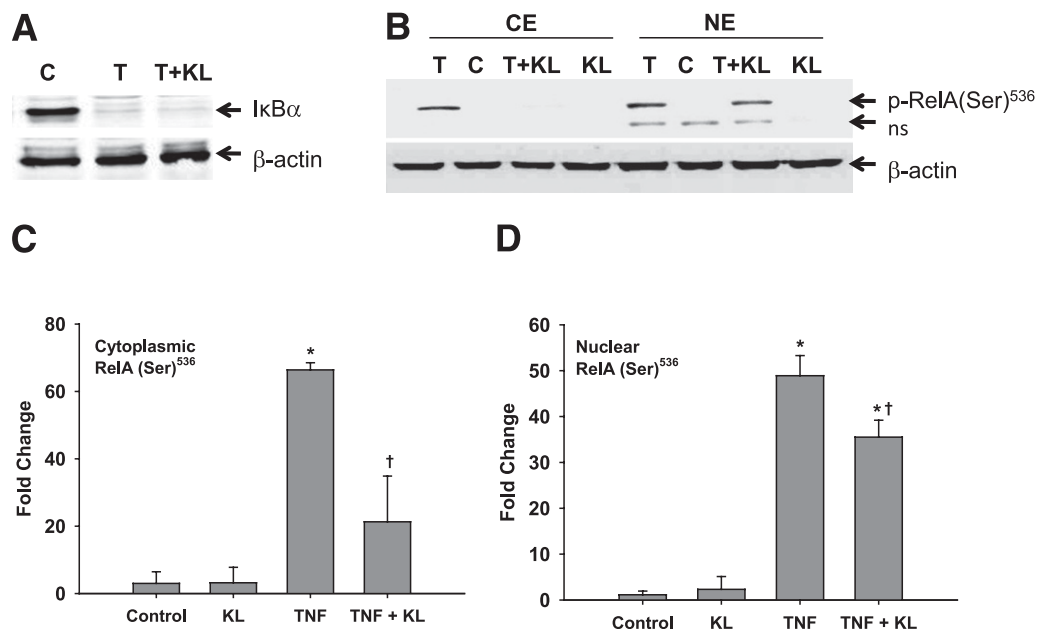


FIG. 6. Mechanism of Klotho (KL)-mediated NF- κ B inhibition. **A:** Immunoblot showing that pretreatment with Klotho (200 pmol/L) did not inhibit TNF- α -induced I κ B α degradation. **Lower panel:** β -Actin was used as the loading control. **B:** Representative Western blot of cytoplasmic extract (CE) and nuclear extract (NE) of HEK293 cells unstimulated or stimulated with TNF- α (T) with or without Klotho pretreated for 45 min. **C and D:** Immunoblots from three independent experiments were quantitated and normalized to respective β -actin and then expressed as fold change vs. control cells. Results show TNF- α -induced increased RelA Ser⁵³⁶ phosphorylation and nuclear translocation of both RelA and RelA Ser⁵³⁶. Klotho blocks only the serine⁵³⁶ phosphorylation. **Lower panel:** β -Actin was used as the loading control. ns, nonspecific. Data represent the means \pm SD of three independent experiments, and overall significance was determined using one-way ANOVA. Significance between groups was analyzed by performing a Turkey post hoc test. * $P < 0.0001$ is significantly different from control samples, whereas $\dagger P < 0.005$ is significantly different from TNF- α -treated samples.

DISCUSSION

The recent characterization of Klotho signaling, an anti-aging hormone that modulates the expression level of antioxidant enzymes, offers a potentially new focus for understanding the accelerated senescence and increased oxidative stress observed in diabetes. Klotho recently has been shown to have renoprotective effects primarily mediated by mitigating mitochondrial oxidative stress and apoptosis (12). In the current study, we have shown a significant decrease of renal Klotho mRNA as well as protein in *db/db* mice compared with age- and sex-matched controls, which is consistent with a recent report (24) of a similar decline of Klotho in kidneys of streptozotocin-induced diabetic rats. In the latter study, the decline in Klotho was linked to hyperglycemia because two pharmacologic approaches to attenuate the severity of hyperglycemia (insulin and phloridzin) restored Klotho levels. We also have reported a novel role for Klotho as a negative modulator of NF- κ B activation via a specific noncanonical activation pathway involving RelA (Ser)⁵³⁶ phosphorylation. These results suggest that Klotho not only confers resistance to oxidative stress (4) but may provide protection against the aberrant activation of NF- κ B pathways. Because Klotho knockout mice exhibit an enhanced aging phenotype, a diabetes-induced decline in Klotho could be an unappreciated mechanism linking increased oxidative stress, inflammation, and accelerated aging in the pathophysiology of diabetic nephropathy.

The concept that diabetes is a chronic inflammatory disease is supported by a rapidly growing array of clinical and experimental data indicating that inflammation, manifested as increases in TNF- α and IL-6, is a common denominator linking obesity, insulin resistance, atherosclerosis, dyslipidemia, and excessive glucose metabolism in diabetes

(25–28). We recently have reported that chronic NF- κ B activation in the renal cortex of *db/db* mice involves a novel mechanism of NF- κ B activation with recruitment of both the canonical and noncanonical NF- κ B pathways (18). In that study, we have shown that multiple proinflammatory cytokines relevant to diabetes, including TNF- α , are increased in the renal cortex of *db/db* mice. We have shown here that Klotho, either expressed transiently as a membranous form or added exogenously in its soluble form, suppresses TNF- α -induced NF- κ B activation and subsequent production of proinflammatory cytokines such as RANTES, MCP-1, IL-6, and IL-8. Our rationale for selecting TNF- α as a diabetic milieu inflammatory stimulus was based on clinical and epidemiological data indicating a role for TNF- α in the initiation and progression of diabetes, including the following: 1) proinflammatory cytokines such as IL-6, TNF- α , IL-1 β , and plasminogen activator inhibitor-1 are increased in diabetic patients and are independently correlated with duration of diabetes (2,29) and 2) acute hyperglycemia increases circulating levels of IL-6, TNF- α , and IL-18 (30,31). Although TNF- α expression in insulin-resistant and in diabetic subjects has been reported to be several-fold higher than in control subjects (28,32), these studies remain controversial. TNF- α plays a permissive role in the development of obesity-induced insulin resistance in mice (33), and numerous tissue culture experiments have demonstrated that glucose, AGEs, and a variety of RAGE ligands increase TNF- α in a variety of cell types (30,34–36). Taken together, these studies indicate that TNF- α is a product of numerous diabetic stimuli and suggest that TNF plays an important upstream role in the activation of NF- κ B observed in diabetes.

There are various regulatory check points for TNF- α -induced canonical NF- κ B pathway activation. Canonical

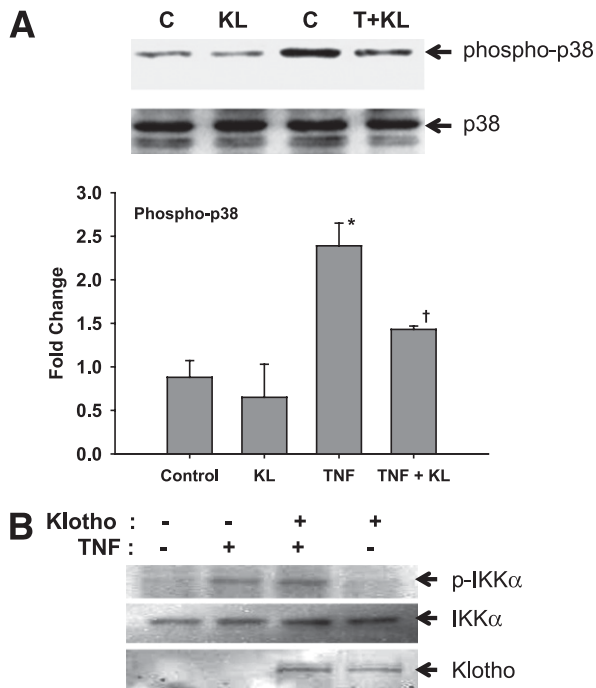


FIG. 7. Klotho decreases p38 phosphorylation. **A:** Western blot showing that pretreatment of Klotho inhibits TNF- α -induced p38 phosphorylation (*left panel*). Immunoblots from three independent experiments were quantitated and normalized to the respective total p38 and then expressed as fold change vs. control cells (*right panel*). Results show that TNF- α -induced increased p38 phosphorylation is significantly reduced by the exogenous addition of Klotho. Data represent the means \pm SD of three independent experiments, and overall significance was determined using one-way ANOVA. Significance between groups was analyzed by performing a Turkey post hoc test. * $P < 0.001$ is significantly different from control samples, whereas † $P < 0.01$ is significantly different from TNF- α -treated samples. C, control; KL, Klotho; T, TNF- α . **B:** Klotho-transfected HEK293 cells were treated with or without TNF- α (20 ng/mL) for 30 min, and whole-cell lysates were immunoblotted with either phospho-IKK α or total IKK α (loading control). *Lower panel:* Expression of transfected Klotho.

NF- κ B proteins (RelA and p50) remain sequestered in the cytoplasm by inhibitors of NF- κ B (such as I κ B) (37). In response to stimuli that activate NF- κ B via the canonical pathway, such as TNF- α , there is activation of the IKK complex; this leads to I κ B α phosphorylation at two specific NH₂-terminal serine residues of the protein, targeting it for ubiquitination and subsequent proteosomal degradation (38,39). This process allows cytoplasmically sequestered RelA p50 dimers to enter the nucleus and bind to NF- κ B promoter sequences to initiate transcription of specific genes. Although Klotho inhibited NF- κ B activation, it did not interfere with TNF- α -induced I κ B α degradation, total RelA nuclear translocation, or DNA binding, suggesting that Klotho might use a novel mechanism of inhibition. Potential possibilities could be inhibition by posttranslational modification of RelA or formation of an active enhanceosome on NF- κ B promoters.

Our findings differ slightly from the recent observations of Maekawa et al. (40). Although both studies report a role for Klotho in modulating NF- κ B activity, the latter study reported that Klotho added exogenously blocked expression of NF- κ B-dependent adhesion molecules by inhibiting I κ B α phosphorylation in response to TNF- α treatment. Several potential reasons for this discrepancy are apparent, including 1) differences in cell type (human umbilical vein endothelial cells vs. renal epithelial cells used in our

study), 2) the unique expression of signaling molecules and distinctive environments of the cultured cells, 3) the source of Klotho, and 4) the relatively high constitutive phosphorylation of I κ B α in the aortic endothelial cell control group. It was surprising that these investigators did not measure total I κ B α degradation or inhibition of RelA nuclear localization by Klotho to buttress their suggestion of NF- κ B canonical pathway inhibition by Klotho.

We have shown that Klotho specifically inhibited TNF- α -induced RelA phosphorylation at Ser⁵³⁶ and its subsequent recruitment on IL-8 and MCP-1 promoters, without affecting total RelA recruitment in response to TNF- α stimulation. RelA (Ser)⁵³⁶ phosphorylation has been shown to occur independently of I κ B α degradation (13,14) and is suggested to be critical for increased NF- κ B transactivation and subsequent activation of a subset of NF- κ B-dependent genes (14). Although the induction of RelA nuclear translocation has been regarded as the main event in NF- κ B pathway activation, more recently the phosphorylation of RelA at various critical Ser residues in its transactivation domain has been proposed as a key event in the activation of NF- κ B signaling (22). The literature suggests that several kinases may phosphorylate the RelA transactivation domain at Ser⁵³⁶ in response to TNF- α and IL-1, including IKKs, PI3K/Akt, TANK-binding kinase-1, and NIK (15,41). NIK, which is induced several-fold in diabetic kidneys, has been reported to induce RelA (Ser)⁵³⁶ phosphorylation directly (13), through p38 mitogen-activated protein kinase (42), or in cooperation with activated Cot (a serine/threonine kinase) (43,44). In addition, overexpression of constitutively active Akt increases RelA transactivation domain phosphorylation in the absence of other stimuli, and pretreatment of cells with LY294002, a PI3K inhibitor, completely blocks this phosphorylation event in response to TNF- α and IL-1 (15,45). Taken together, these results clearly suggest involvement of PI3K/Akt in TNF- α /IL-1-induced RelA (Ser)⁵³⁶ phosphorylation and subsequent NF- κ B activation. Akt has been proposed to mediate RelA phosphorylation by activating p38 and requiring both IKKs, IKK α and IKK β (23). Because we did not observe an inhibitory effect of Klotho on TNF- α -induced I κ B α degradation, we reasoned that IKK β , which is a potent inducer of I κ B α phosphorylation and its subsequent degradation, may not be a target of Klotho. Likewise, TANK-binding kinase-1, which is an IKK-related kinase but not a part of the IKK complex and not required for I κ B α phosphorylation and degradation, can phosphorylate RelA at Ser⁵³⁶ in response to TNF- α treatment (46,47). Thus, it is possible that Klotho may unleash its anti-inflammatory effects by blocking NF- κ B activation through inhibiting the PI3K/Akt, IKK α , or NIK activation normally seen after TNF- α treatment. Our finding that Klotho blocks p38 phosphorylation is consistent with earlier observations that Klotho blocks basal or insulin-induced Akt phosphorylation (4). It will be important to identify the RelA transactivation domain kinase, which is sensitive to Klotho to understand how Klotho suppresses this noncanonical RelA activation pathway and how its loss contributes to the renal inflammation associated with diabetic nephropathy.

In conclusion, we have established that Klotho has an anti-inflammatory function in the kidney in addition to its ability to engender resistance to oxidative stress. Thus, an adequate tissue level of Klotho may provide dual protection against both oxidative stress and inflammation, while loss of Klotho may be a common denominator linking increased oxidative stress, NF- κ B activation, and accelerated aging in diabetes.

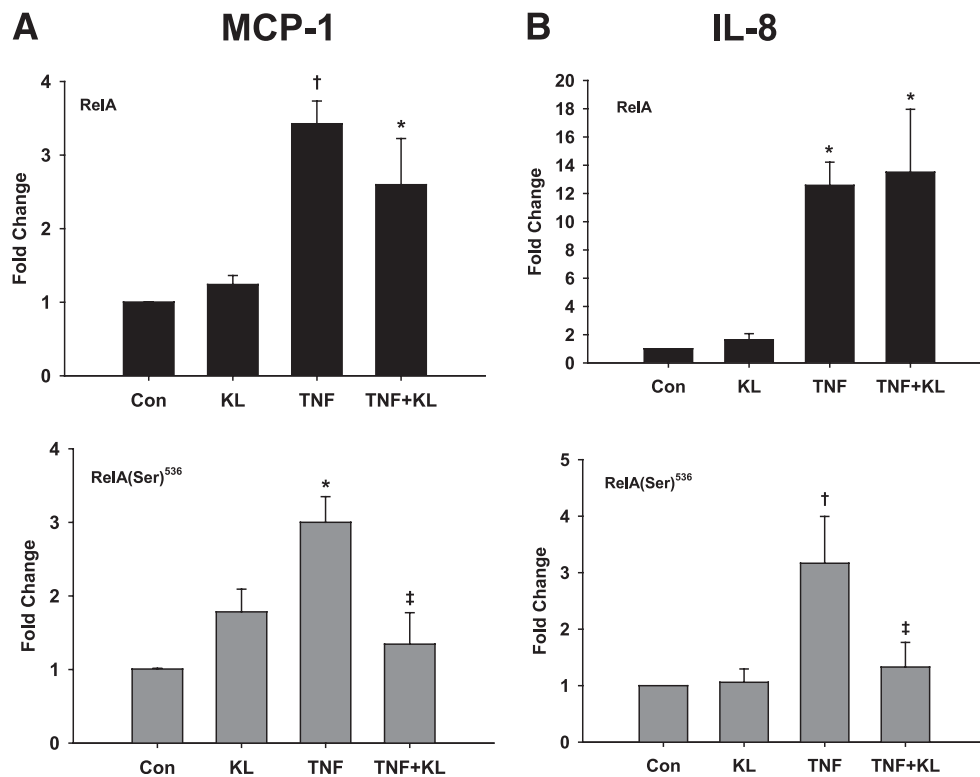


FIG. 8. Klotho inhibits recruitment of RelA Ser⁵³⁶ on IL-8 and MCP-1 promoters. HEK293 cells were pretreated with Klotho (KL) alone or in combination with TNF- α (T) (20 ng/mL for 30 min), cross-linked, and sonicated, and the recruitment of RelA and RelA Ser⁵³⁶ on IL-8 (A) and MCP-1 (B) promoters was examined by performing a ChIP assay. DNA pulled down with the respective antibody was used for quantitative RT-PCR using ChIP-specific primer sets. Data were normalized to internal control, GAPDH, and were expressed as fold change compared with the respective untreated cells. Data represent the means \pm SD of three independent experiments, which were analyzed by one-way ANOVA followed by assessment of significance between groups using a Turkey post hoc test. * $P < 0.005$ and † $P < 0.0005$ are significantly different from control (Con) samples; ‡ $P < 0.005$ is significantly different from the TNF-treated sample.

ACKNOWLEDGMENTS

This work was supported by a grant to S.C. and R.G.T. from the National Institutes of Health (NIH), National Institute of Diabetes and Digestive and Kidney Diseases (R01-DK-079053) and a grant to S.C. from the American Heart Association (0630100N). K.P.R. also was supported by an NIH National Heart, Lung, and Blood Institute Grant (NO1-HV-28184), a Welch Foundation Endowment in Chemistry and Related Science Grant (L-AU-0002), an American Diabetes Association Grant (1-08-CR-65), and an NIH Clinical and Translational Award (UL1-RR-024148-05).

No potential conflicts of interest relevant to this article were reported.

Y.Z., S.B., and N.D. performed the experiments. W.S.L. contributed to animal handling and mouse renal primary tubular epithelial cell isolation. P.S.S. researched data and contributed to discussion. R.B. prepared the expression plasmids and purified the Klotho protein. K.P.R. contributed to data analysis and discussion and reviewed and edited the manuscript. R.G.T. designed the animal studies, analyzed data, contributed to discussion, and reviewed and edited the manuscript. S.C. researched and analyzed data, contributed to discussion, and wrote the manuscript.

The authors thank Allan Brasier, University of Texas Medical Branch, Galveston, TX, for his helpful discussions concerning the approaches used in this study and his expertise in the field of NF- κ B activation and inflammation. The authors also acknowledge the assistance of Heidi Sprat, University of Texas Medical Branch, Galveston, TX, with statistical analyses.

REFERENCES

- Mazza AD, Morley JE. Update on diabetes in the elderly and the application of current therapeutics. *J Am Med Dir Assoc* 2007;8:489–492
- Verzola D, Gandolfo MT, Gaetani G, et al. Accelerated senescence in the kidneys of patients with type 2 diabetic nephropathy. *Am J Physiol Renal Physiol* 2008;295:F1563–F1573
- Kuro-o M. Klotho as a regulator of oxidative stress and senescence. *Biol Chem* 2008;389:233–241
- Yamamoto M, Clark JD, Pastor JV, et al. Regulation of oxidative stress by the anti-aging hormone klotho. *J Biol Chem* 2005;280:38029–38034
- Biber J, Hernando N, Forster I, Murer H. Regulation of phosphate transport in proximal tubules. *Pflugers Arch* 2009;458:39–52
- Hu MC, Shi M, Zhang J, et al. Klotho: a novel phosphaturic substance acting as an autocrine enzyme in the renal proximal tubule. *FASEB J* 2010;24:3438–3450
- Kuro-o M, Matsumura Y, Aizawa H, et al. Mutation of the mouse klotho gene leads to a syndrome resembling ageing. *Nature* 1997;390:45–51
- Kurosu H, Yamamoto M, Clark JD, et al. Suppression of aging in mice by the hormone Klotho. *Science* 2005;309:1829–1833
- Masuda H, Chikuda H, Suga T, Kawaguchi H, Kuro-o M. Regulation of multiple ageing-like phenotypes by inducible klotho gene expression in klotho mutant mice. *Mech Ageing Dev* 2005;126:1274–1283
- Koh N, Fujimori T, Nishiguchi S, et al. Severely reduced production of klotho in human chronic renal failure kidney. *Biochem Biophys Res Commun* 2001;280:1015–1020
- Sugiura H, Yoshida T, Tsuchiya K, et al. Klotho reduces apoptosis in experimental ischaemic acute renal failure. *Nephrol Dial Transplant* 2005;20:2636–2645
- Haruna Y, Kashihara N, Satoh M, et al. Amelioration of progressive renal injury by genetic manipulation of Klotho gene. *Proc Natl Acad Sci USA* 2007;104:2331–2336
- Choudhary S, Lu M, Cui R, Brasier AR. Involvement of a novel Rac/RhoA guanosine triphosphatase-nuclear factor-kappaB inducing kinase signaling pathway mediating angiotensin II-induced RelA transactivation. *Mol Endocrinol* 2007;21:2203–2217

14. Cui R, Tieu B, Recinos A, Tilton RG, Brasier AR. RhoA mediates angiotensin II-induced phospho-Ser536 nuclear factor kappaB/RelA subunit exchange on the interleukin-6 promoter in VSMCs. *Circ Res* 2006;99:723–730
15. Sizemore N, Leung S, Stark GR. Activation of phosphatidylinositol 3-kinase in response to interleukin-1 leads to phosphorylation and activation of the NF-kappaB p65/RelA subunit. *Mol Cell Biol* 1999;19:4798–4805
16. Cunningham R, Steplock D, Wang F, et al. Defective parathyroid hormone regulation of NHE3 activity and phosphate adaptation in cultured NHERF-1/-renal proximal tubule cells. *J Biol Chem* 2004;279:37815–37821
17. Duran-Jimenez B, Dobler D, Moffatt S, et al. Advanced glycation end products in extracellular matrix proteins contribute to the failure of sensory nerve regeneration in diabetes. *Diabetes* 2009;58:2893–2903
18. Starkey JM, Haidacher SJ, LeJeune WS, et al. Diabetes-induced activation of canonical and noncanonical nuclear factor- κ B pathways in renal cortex. *Diabetes* 2006;55:1252–1259
19. Livak KJ, Schmittgen TD. Analysis of relative gene expression data using real-time quantitative PCR and the 2(-Delta Delta C(T)) Method. *Methods* 2001;25:402–408
20. Hou T, Ray S, Lee C, Brasier AR. The STAT3 NH2-terminal domain stabilizes enhanceosome assembly by interacting with the p300 bromodomain. *J Biol Chem* 2008;283:30725–30734
21. Zhang H, Li Y, Fan Y, et al. Klotho is a target gene of PPAR-gamma. *Kidney Int* 2008;74:732–739
22. Neumann M, Naumann M. Beyond IkappaBs: alternative regulation of NF-kappaB activity. *FASEB J* 2007;21:2642–2654
23. Madrid LV, Mayo MW, Reuther JY, Baldwin AS Jr. Akt stimulates the transactivation potential of the RelA/p65 Subunit of NF-kappa B through utilization of the Ikappa B kinase and activation of the mitogen-activated protein kinase p38. *J Biol Chem* 2001;276:18934–18940
24. Cheng MF, Chen LJ, Cheng JT. Decrease of Klotho in the kidney of streptozotocin-induced diabetic rats. *J Biomed Biotechnol* 2010;2010:513853
25. Monroy A, Kamath S, Chavez AO, et al. Impaired regulation of the TNF-alpha converting enzyme/tissue inhibitor of metalloproteinase 3 proteolytic system in skeletal muscle of obese type 2 diabetic patients: a new mechanism of insulin resistance in humans. *Diabetologia* 2009;52:2169–2181
26. Federici M, Hribal ML, Menghini R, et al. Timp3 deficiency in insulin receptor-haploinsufficient mice promotes diabetes and vascular inflammation via increased TNF-alpha. *J Clin Invest* 2005;115:3494–3505
27. Navarro-Gonzalez J, Mora-Fernandez C, Gomez-Chinchon M, Muros M, Herrera H, Garcia J. Serum and gene expression profile of tumor necrosis factor-alpha and interleukin-6 in hypertensive diabetic patients: effect of amlodipine administration. *Int J Immunopathol Pharmacol* 2010;23:51–59
28. Saghizadeh M, Ong JM, Garvey WT, Henry RR, Kern PA. The expression of TNF alpha by human muscle. Relationship to insulin resistance. *J Clin Invest* 1996;97:1111–1116
29. Pickup JC, Chusney GD, Thomas SM, Burt D. Plasma interleukin-6, tumour necrosis factor alpha and blood cytokine production in type 2 diabetes. *Life Sci* 2000;67:291–300
30. Morohoshi M, Fujisawa K, Uchimura I, Numano F. Glucose-dependent interleukin 6 and tumor necrosis factor production by human peripheral blood monocytes in vitro. *Diabetes* 1996;45:954–959
31. Esposito K, Nappo F, Marfella R, et al. Inflammatory cytokine concentrations are acutely increased by hyperglycemia in humans: role of oxidative stress. *Circulation* 2002;106:2067–2072
32. Lorenzo M, Fernández-Veledo S, Vila-Bedmar R, Garcia-Guerra L, De Alvaro C, Nieto-Vazquez I. Insulin resistance induced by tumor necrosis factor-alpha in myocytes and brown adipocytes. *J Anim Sci* 2008;86 (Suppl.):E94–E104
33. Uysal KT, Wiesbrock SM, Marino MW, Hotamisligil GS. Protection from obesity-induced insulin resistance in mice lacking TNF-alpha function. *Nature* 1997;389:610–614
34. Rashid G, Korzets Z, Bernheim J. Advanced glycation end products stimulate tumor necrosis factor-alpha and interleukin-1 beta secretion by peritoneal macrophages in patients on continuous ambulatory peritoneal dialysis. *Isr Med Assoc J* 2006;8:36–39
35. Webster L, Abordo EA, Thornalley PJ, Limb GA. Induction of TNF alpha and IL-1 beta mRNA in monocytes by methylglyoxal- and advanced glycated endproduct-modified human serum albumin. *Biochem Soc Trans* 1997;25:250S
36. Wang AL, Yu ACH, He QH, Zhu X, Tso MOM. AGEs mediated expression and secretion of TNF alpha in rat retinal microglia. *Exp Eye Res* 2007;84:905–913
37. Siebenlist U, Franzoso G, Brown K. Structure, regulation and function of NF-kappa B. *Annu Rev Cell Biol* 1994;10:405–455
38. Hayden MS, Ghosh S. Signaling to NF-kappaB. *Genes Dev* 2004;18:2195–2224
39. Ghosh S, Baltimore D. Activation in vitro of NF-kappa B by phosphorylation of its inhibitor I kappa B. *Nature* 1990;344:678–682
40. Maekawa Y, Ishikawa K, Yasuda O, et al. Klotho suppresses TNF-alpha-induced expression of adhesion molecules in the endothelium and attenuates NF-kappaB activation. *Endocrine* 2009;35:341–346
41. Yang F, Tang E, Guan K, Wang CY. IKK beta plays an essential role in the phosphorylation of RelA/p65 on serine 536 induced by lipopolysaccharide. *J Immunol* 2003;170:5630–5635
42. Jijon H, Allard B, Jobin C. NF-kappaB inducing kinase activates NF-kappaB transcriptional activity independently of IkappaB kinase gamma through a p38 MAPK-dependent RelA phosphorylation pathway. *Cell Signal* 2004;16:1023–1032
43. Wittwer T, Schmitz ML. NIK and Cot cooperate to trigger NF-kappaB p65 phosphorylation. *Biochem Biophys Res Commun* 2008;371:294–297
44. Kane LP, Mollenauer MN, Xu Z, Turck CW, Weiss A. Akt-dependent phosphorylation specifically regulates Cot induction of NF-kappa B-dependent transcription. *Mol Cell Biol* 2002;22:5962–5974
45. Wang D, Westerheide SD, Hanson JL, Baldwin AS Jr. Tumor necrosis factor alpha-induced phosphorylation of RelA/p65 on Ser529 is controlled by casein kinase II. *J Biol Chem* 2000;275:32592–32597
46. Kishore N, Huynh QK, Mathialagan S, et al. IKK-i and TBK-1 are enzymatically distinct from the homologous enzyme IKK-2: comparative analysis of recombinant human IKK-i, TBK-1, and IKK-2. *J Biol Chem* 2002;277:13840–13847
47. Fujita F, Taniguchi Y, Kato T, et al. Identification of NAP1, a regulatory subunit of IkappaB kinase-related kinases that potentiates NF-kappaB signaling. *Mol Cell Biol* 2003;23:7780–7793